



ARTIFICIAL INTELLIGENCE

Prediction of manifest refraction using machine learning ensemble models on wavefront aberrometry data

Carlos S. Hernández^{a,b,c}, Andrea Gil^{a,b,c}, Ignacio Casares^{a,c}, Jesús Poderoso^{a,c}, Alec Wehse^b, Shivang R. Dave^b, Daryl Lim^b, Manuel Sánchez-Montañés^d, Eduardo Lage^{a,b,c,*}

^a Department of Electronics and Communications Technology, Escuela Politécnica Superior, Universidad Autónoma de Madrid, Spain

^b PlenOptika, Inc., Boston, MA, USA

^c Instituto de Investigación Sanitaria Fundación Jiménez Díaz, Madrid, Spain

^d Department of Computer Science. Escuela Politécnica Superior, Universidad Autónoma de Madrid, Spain

KEYWORDS

Machine learning;
Subjective refraction;
Wavefront aberrometry;
Portable autorefractor

Abstract

Purpose: To assess the performance of machine learning (ML) ensemble models for predicting patient subjective refraction (SR) using demographic factors, wavefront aberrometry data, and measurement quality related metrics taken with a low-cost portable autorefractor.

Methods: Four ensemble models were evaluated for predicting individual power vectors (M , J_0 , and J_{45}) corresponding to the eyeglass prescription of each patient. Those models were random forest regressor (RF), gradient boosting regressor (GB), extreme gradient boosting regressor (XGB), and a custom assembly model (ASB) that averages the first three models. Algorithms were trained on a dataset of 1244 samples and the predictive power was evaluated with 518 unseen samples. Variables used for the prediction were age, gender, Zernike coefficients up to 5th order, and pupil related metrics provided by the autorefractor. Agreement with SR was measured using Bland-Altman analysis, overall prediction error, and percentage of agreement between the ML predictions and subjective refractions for different thresholds (0.25 D, 0.5 D).

Results: All models considerably outperformed the predictions from the autorefractor, while ASB obtained the best results. The accuracy of the predictions for each individual power vector component was substantially improved resulting in $a \pm 0.63$ D, ± 0.14 D, and ± 0.08 D reduction in the 95% limits of agreement of the error distribution for M , J_0 , and J_{45} , respectively. The wavefront-aberrometry related variables had the biggest impact on the prediction, while demographic and measurement quality-related features showed a heterogeneous but consistent predictive value.

* Corresponding author at: Department of Electronics and Communications Technology, Escuela Politécnica Superior, Universidad Autónoma de Madrid, Spain.

E-mail address: eduardo.lage@uam.es (E. Lage).

<https://doi.org/10.1016/j.optom.2022.03.001>

1888-4296/© 2022 Spanish General Council of Optometry. Published by Elsevier España, S.L.U. This is an open access article under the CC BY license (<http://creativecommons.org/licenses/by/4.0/>).

Conclusions: These results suggest that ML is effective for improving precision in predicting patient's SR from objective measurements taken with a low-cost portable device.

© 2022 Spanish General Council of Optometry. Published by Elsevier España, S.L.U. This is an open access article under the CC BY license (<http://creativecommons.org/licenses/by/4.0/>).

Introduction

According to the Vision Loss Expert Group (VLEG), it is expected that 1.7 billion people will be affected by moderate or severe vision impairment by 2050,¹ the lead cause being uncorrected refractive errors (URE).² URE is a reversible condition that carries significant individual and societal costs.³ For people suffering from URE, sight can be restored with refractive surgery, contact lenses, or with appropriate eyeglasses, the latter being one of the most cost-effective healthcare solutions.⁴ Despite the strong impetus to correct UREs and given their impact on achieving the United Nations (UN) Sustainable Development Goals (SDGs), they surprisingly remain historically underfunded relative to other diseases of the eye.⁵ Their prevalence remains high, particularly in low- and middle-income countries (LMICs), where vision exams can be highly inaccessible due to a shortage of eyecare professionals (ECPs) capable of providing clinical-quality eyeglass prescriptions.

The gold standard for prescribing eyeglasses is subjective, or manifest refraction. This is a time-consuming procedure that starts with an objective assessment of the refractive error by means of retinoscopy (in low-resource settings) or autorefractometry (in high-resource settings), followed by a subjective refinement until the best corrected visual acuity is obtained. Accuracy of manifest refraction heavily relies on the experience of an ECP and the comprehension and visual perception of the subject. Repeatability of refractive error measurements in clinical settings has a high degree of variability that has been reported to range from 0.16 D to over 0.78 D in spherical equivalent (average differences).^{6,7}

Wavefront aberrometry is an objective method for measuring refractive power. It provides a detailed map of the eye containing a description of both low- (LOA) and high-order (HOA) aberrations. The shape of the aberrated wavefront is commonly described using the Zernike polynomials, the standard method to represent the error in the wavefront of an optical system with circular pupil.⁸ Wavefront aberrometers have demonstrated high accuracy⁹ and higher repeatability than manifest refraction,^{10,11} but they continue to fail to match the gold standard. These discrepancies have been associated with several phenomena such as inter-ECP variability,⁶ influence of high-order aberrations,^{12,13} effects of iris color on the infrared light employed in wavefront aberrometry,¹⁴ accommodation during the measurement,¹⁵ or neural compensation of the refractive error.^{16,17}

The relationship between the optical image on the retina and human visual perception continues to be a primary focus in vision research. Computational approaches attempting to predict subjective refraction from wavefront aberrometry data using retinal image quality metrics,^{12,13,18} or novel wavefront fitting methods,¹⁹ have proven to perform better than standard pupil plane metrics, yet continue to generally

not be considered accurate enough to substitute the gold standard.²⁰

During the past few years, ML algorithms have experienced an exponential boost in performance, accuracy, and community support.²¹ In the field of optometry, ML has been employed to predict subjective refraction using the Zernike coefficients with deep learning techniques²² or using extreme gradient boosting with a new series of polynomials for describing the wavefront map.^{23,24} These approaches, which are largely at research stage, have shown that significant improvements in accuracy can be achieved when using aberrometry data obtained by benchtop systems in highly controlled clinical and research environments. Unfortunately, such cost-prohibitive requirements fail to address the access barriers faced by healthcare disparities populations. Furthermore, refractive errors are also known to be correlated to demographic factors (particularly age),²⁵ that can be interpreted by the models and potentially used to improve prediction power.

The primary aim of this work was to assess the performance of different machine learning ensemble models to predict patient subjective refraction using wavefront aberrometry and demographic variables. In contrast with the previous studies, data used for this work was obtained from a clinical study performed in 2015 at Aravind Eye Hospital in Madurai and a rural satellite vision center in Thiruppuvanam, India. The objective of that study was to evaluate the quality of eyeglass prescriptions provided by a low-cost portable wavefront autorefractor,²⁶ an early prototype of the QuickSee (QS) (PlenOptika Inc, USA), operated by a minimally trained technician in a low-resource setting on a population with high age and refractive error variability. The secondary aim of this study was to understand if ML-based approaches, when applied to real-world data obtained with low-cost handheld ophthalmic devices could potentially increase access to accurate, clinical-quality SR prescriptions when operated by non-experts.

Materials and methods

Dataset description

A total of 708 subjects were enrolled in the study, 506 from the base hospital (HA) and 202 from the vision center (VA). Inclusion criteria were patients with ages ranging between 15 and 70 years and within the measurement range of the device used in the study (spherical equivalent of -6 D to $+10$ D). Exclusion criteria included presence of mature cataract, any prior eye surgery, any major eye illnesses, and use of systemic or ocular drugs which may affect vision. Subjective refraction results, QS measurements, and demographic data were recorded for all subjects eligible for the study. Clinical refraction procedure included streak retinoscopy and subjective refraction by an experienced refractionist. Further details about the study protocols can be found in Durr

et al.²⁶ Patients with missing data, like age or gender, or with the presence of cataract or other problem that prevented the autorefractor from providing a reliable prescription were removed from the dataset.

Autorefractor

One distinctive feature of QS compared to standard desktop autorefractors is that it works in video mode. Instead of providing an eyeglass prescription from a single wavefront image (or the average of several static images), it records a large sequence of Shack-Hartmann spot patterns over a 10 s video and applies advanced algorithms to process the sequence.²⁷ Consequently, this device can provide not only standard aberrometry results (Zernike coefficients), but also a set of measurement-related quality metrics, such as the standard deviations of pupil size and pupil center in X and Y directions during the acquisition, which were also used for training the different models. Additional information about the device working principle can be found here.²⁸

Machine learning models

Although in the original study 3 measurements for each eye were acquired, in this work only the first measurement of each eye was used to avoid training the ML algorithms with redundant data. To account for instances where there were significant differences between the 3 different

measurements of each eye, one of the two additional measurements were included in the dataset. The threshold to include this additional data was a spherical equivalent difference of $\geq 0.5D$ between the three measurements (standard deviation $\geq 0.5D$) of the same eye. Of the two additional measurements, the one with the biggest difference from the first measurement was selected. Consequently, each patient contributed a minimum of 2 measurements (1 per eye) and a maximum of 4 measurements (2 per eye).

Choosing the proper number of observations to be used for training and testing does not follow a general rule. In our case, due to the relatively small dataset, it was decided to use 70% of the subjects for training and the remaining 30% for testing. Partitioning was performed using stratified sampling to ensure similar distributions of age, gender, and spherical equivalent error between all sets. As an additional validation step, all measurements for both eyes for a given patient were placed either in training or testing to prevent information leakage.

The performance of the ML models is known to be very sensitive to the quality and number of features considered for predictions.²⁹ Redundant or unrelated variables can reduce the accuracy of the models and increase its complexity causing overfitting. In this work, we only employed prediction variables known to influence subjective refraction Table 1. provides a description of the variables employed to train the models as well as the rationale behind the decision.

Table 1 Description and justification of the wavefront aberrometry, measurement quality metrics, and demographic variables used to train the models.

	Variable Name	Description	Justification
Wavefront Aberrometry	$[Z_2^{-2}, \dots, Z_5^5]$	Zernike coefficients up to 5th order without the Piston, Tilt, and Tip since they are not used for computation of low- and high-order aberrations.	Zernike coefficients are the standard method to describe the optical aberrations of the eye. ⁸
Measurement quality metrics	[PS_Avg]	Average pupil size along the 10 s measurement.	Pupil size strongly influences magnitude of HOAs. ³⁶
	[PS_Std]	Standard deviation of pupil size along the 10 s measurement with the QS prototype.	Changes in pupil size are usually related to accommodation. ³⁷
Demographic	[PC_Std_X, PC_Std_Y]	Standard deviation of the center of the pupil in X and Y directions during the measurement.	Misalignments between the eye and Shack-Hartman sensor will capture (and refract) the periphery of the pupil. Central and peripheral refractions can be different in some populations. ^{38,39}
	[Age]	Patient's age.	Prevalence of refractive errors ²⁵ and accommodation range ⁴⁰ are strongly correlated to age.
	[Gender]	Patient's gender.	Prevalence of refractive errors has been reported to have some degree of correlation with gender. ^{41,42}

Specifically, input features were separated into aberrometry data, measurement quality related metrics, and demographic data.

Four ensemble models were trained and tested for each power vector component: random forest regressor^{30,31} (RF), gradient boosting regressor^{30–32} (GB), extreme gradient boosting regressor³³ (XGB), and a custom assembly model (ASB) that averages the predictions of RF, GB and XGB. Ensemble regression techniques, like averaging the output of several models, are known to reduce the variance of the final prediction.³¹ Since selection of the best model is linked to the selection of the best features, we performed an extensive grid search; for each combination of input features, each model underwent hyperparameter tuning using a 5-fold randomized cross-validation using the mean absolute error as scoring function. The impact of individual features in the predictions of the models was estimated using permutation-based algorithms. Permutation values were also obtained using 5-fold cross-validation in the training set.

The research code was developed in JupyterLab (2.1.5) IDE using Python (3.8.3). Data preprocessing, aggregation, and cleaning in preparation for machine learning was implemented with Pandas (1.0.5) and Numpy (1.18.5). Machine learning models Random Forest and Gradient Boosting were from Scikit-learn (0.23.1) and Extreme Gradient Boosting from XGBoost (1.2.1).

Statistical analysis

Statistical analysis was performed on the power vector domain using the predictions from ML models and the autorefractor on the test dataset. Subjective refraction prescriptions were converted to power vector parameters of spherical equivalent (M), vertical Jackson cross cylinder (J_0), and oblique Jackson cross cylinder (J_{45}).³⁴ In the original study,²⁵ samples used for statistical analysis were the median of three measurements for the right eye. This differs from the analysis in this paper, in which we used individual measurements from both eyes for the calculations.

Three statistical procedures were followed to measure agreement between predictions and subjective refraction. First, Bland-Altman analysis was performed since it is the standard procedure when evaluating the accuracy and precision of two separate measurement methods (in this case, predicted refraction compared to subjective

refraction).³⁵ Second, overall prediction error was measured in terms of mean absolute error (MAE) and root mean squared error (RMSE), a metric more sensitive to outliers. Finally, we evaluated the percentage of agreement between predictions and subjective refraction for 0.25 D and 0.5 D thresholds.

Results

Population

After data preprocessing and cleaning, 669 subjects (94.5% of overall patient dataset) remained for the analysis. A demographic description and distribution of spherical equivalent errors of the patient population is reported in Table 2 and Fig. 1, respectively. The proportion of age, gender, and spherical equivalent is comparable between training and testing groups.

Agreement with subjective refraction

The four algorithms performed similarly, but the ASB model (formed by the mean of the predictions of RF, GB, and XGB) slightly reduced the error, while keeping the same percentage of agreement as the other three models. Therefore, the results discussed below will all refer to the ASB model. Detailed results for each model are shown in summary Table 3.

ASB model significantly improved the agreement with subjective refraction compared to the baseline autorefractor results. The mean absolute error (MAE) decreased by 42.5% (0.27 D), 29.4% (0.06 D), and 41.7% (0.05 D), for M, J_0 , and J_{45} , respectively. The RMSE was also reduced in similar proportions (38.1% (0.32 D), 29.2% (0.08 D), and 23.5% (0.04 D), for M, J_0 , and J_{45} , respectively). In terms of percentage of agreement between predictions and SR, the proportion of outliers (≥ 1 D) in the spherical equivalent predictions was reduced from 20.3% in the baseline model to 5.2% in the ASB model. Furthermore, the percentage of agreement for a 0.5 D threshold increased from 44.8% (QS-SR) to 72.9% (ML-SR) for spherical equivalent refraction.

Fig. 2 contains a histogram of the prediction error of ASB and QS models for the three power vectors. The plots show the effect in prediction accuracy and precision of the machine learning model. The general trend to underestimate the M value in the baseline model was mostly

Table 2 Population demographics characteristics and spherical equivalent error distribution.

Characteristics	Entire Dataset	Training Set	Testing Set	T test (p-value) Training vs Testing
Number of Subjects	669	468	201	–
Number of Samples	1762	1244	518	–
Female n (%)	391 (58.4)	269 (57.5)	122 (60.7)	0.31
Age \pm SD (range) [years]	35.2 \pm 13.7 (15 - 70)	35.5 \pm 13.6 (15 - 70)	34.5 \pm 13.7 (16 - 64)	0.15
SE \pm SD (range) [diopters]	–0.7 \pm 1.67 (–6.0 - 3.5)	–0.67 \pm 1.62 (–5.75 - 3.5)	–0.83 \pm 1.77 (–6.0 - 2.63)	0.06

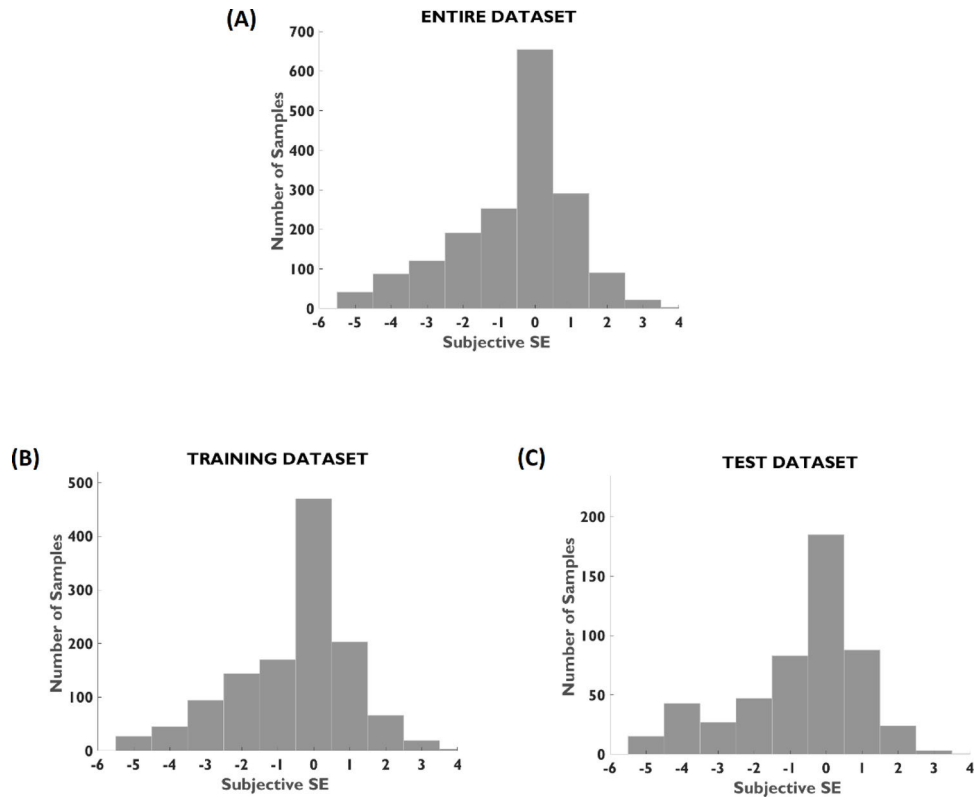


Fig. 1 Distribution of spherical equivalent errors in patient population. (A) Entire dataset, (B) training dataset, and (C) testing dataset. Histograms bin size is 1.0 D. Refraction data was obtained by standard subjective procedure.

corrected by the ASB model, but the percentage of overestimation was similar in both cases.

Bland-Altman analysis showed a bias between ASB and SR predictions of 0.15 D, -0.01 D, and 0.01 D, for M , J_0 , and

J_{45} , respectively (Fig. 3). The 95% limits of agreement (calculated as 1.96 x Standard Deviation of the differences) between ASB and SR were ± 0.99 D, ± 0.33 D, and ± 0.25 D, for M , J_0 , and J_{45} . Compared to the Bland-Altman diagram of

Table 3 Agreement comparison between ML models predictions and autorefractor with subjective refraction for M , J_0 , and J_{45} . ASB model provided the best results for the three power vectors. *LOA: Limits of agreement calculated as 1.96 x Standard Deviation of the differences.

Model		Objective Dynamic + Demographic Features						Bland-Altman (D)	
		MAE	RMSE	Min.	Max.	Agreement (%)			
QS	M	0.65	0.84	-3.19	2.33	25.87%	44.79%	Mean	95% LOA
	J_0	0.17	0.24	-1.59	0.99	76.25%	96.71%	0.01	-1.75, +1.49
	J_{45}	0.12	0.17	-0.63	0.68	88.22%	98.45%	0.02	-0.47, +0.48
RF	M	0.39	0.54	-1.70	2.45	45.17%	72.01%	0.17	-0.31, +0.34
	J_0	0.13	0.17	-0.81	0.69	88.80%	97.88%	0.00	-0.83, +1.17
	J_{45}	0.07	0.13	-0.81	0.87	94.02%	99.23%	0.01	-0.34, +0.34
GB	M	0.40	0.54	-1.55	2.29	41.50%	69.31%	0.13	-0.24, +0.26
	J_0	0.13	0.17	-0.71	0.75	89.18%	98.26%	-0.01	-0.88, 1.15
	J_{45}	0.07	0.13	-0.88	0.99	94.40%	99.23%	0.00	-0.35, +0.32
XGB	M	0.40	0.53	-1.70	2.66	44.01%	71.62%	0.15	-0.25, +0.25
	J_0	0.12	0.17	-0.71	0.74	89.58%	98.06%	0.00	-0.86, +1.15
	J_{45}	0.07	0.14	-0.88	0.99	94.59%	98.46%	0.01	-0.34, +0.33
ASB	M	0.38	0.52	-1.55	2.40	45.56%	72.90%	0.15	-0.26, +0.28
	J_0	0.11	0.16	-0.74	0.72	89.10%	98.64%	-0.01	-0.83, +1.13
	J_{45}	0.07	0.13	-0.81	0.97	95.27%	99.23%	0.01	-0.34, +0.32

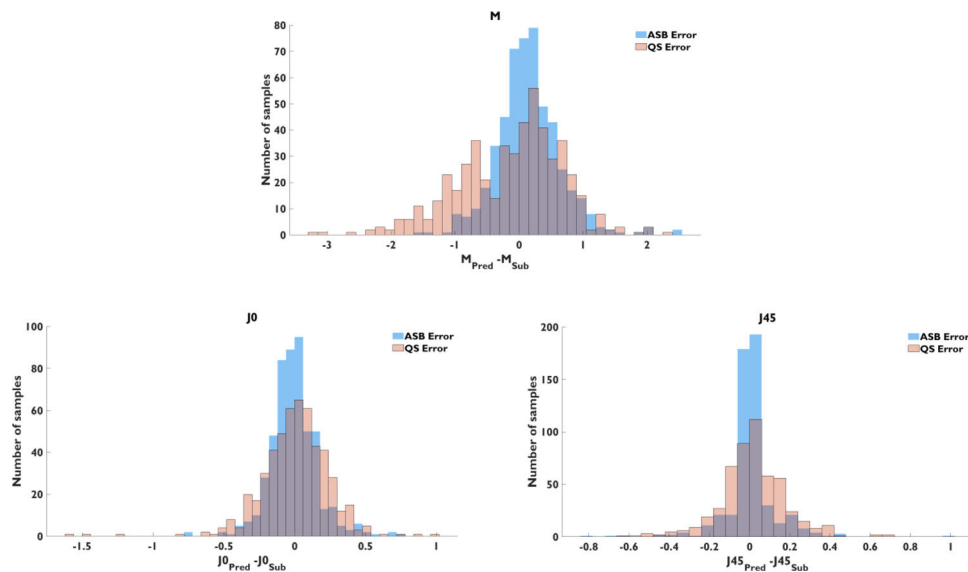


Fig. 2 Distribution of the prediction error for M , J_0 , and J_{45} of the assembly model (blue) and autorefractor (orange).

the baseline model, the 95% limits of agreement of predictions were reduced by ± 0.63 D, ± 0.14 D, and ± 0.08 D, for M , J_0 , and J_{45} .

Fitting a linear regression model to each Bland-Altman (Fig. 3) provided a slope of -0.12 , -0.11 , and -0.40 , for M , J_0 , and J_{45} , for the assembly model, compared to a slope of 0.31 , 0.35 , and 0.30 , for M , J_0 , and J_{45} , for the autorefractor predictions. The change in slope sign indicates a trend for under correction of the ASB model in both myopic and hyperopic regions, and the flattening of the slope for the spherical equivalent indicates higher agreement with SR in the edges of both measurement ranges. Bland-Altman plots for the different power vector components (Fig. 3) clearly shows this change in the distribution of the differences and its effect in the 95% limits of agreement, which are considerably improved in all the cases.

Feature importance

In general, for all the models evaluated the most relevant features for predicting individual power vectors were Zernike coefficients Z_2^0 (defocus), Z_2^2 (vertical astigmatism), average pupil size, and age for spherical equivalent; Zernike coefficient Z_2^2 (vertical astigmatism), average pupil size, and age for vertical Jackson cross cylinder (J_0); and Zernike coefficients Z_2^{-2} (oblique astigmatism), Z_2^2 (vertical astigmatism), average pupil size, average deviation in pupil center and age for oblique Jackson cross cylinder (J_{45}) (Fig. 4).

The three base models provided different levels of importance to each feature but demonstrated agreement on the most relevant parameters. Regarding the demographic variables, the age was in general an important piece of information for all the power vector components being predicted, while gender was found to be practically irrelevant. Measurement quality metrics included were relevant in the prediction, especially the average pupil size, which was of interest for all the models, and

the standard deviation of the pupil center was of interest for J_{45} models.

Conclusions

This study evaluated the prediction power of four different machine learning ensemble models to estimate manifest refraction from wavefront aberrometry data, demographic factors, and measurement-quality metrics. Agreement with subjective refraction for M , J_0 , and J_{45} was considerably improved compared to the baseline results provided by the autorefractor. Similarly, the variance of the predictions (95% limits of agreement) was reduced for the three power vector components while keeping the bias error close to zero. This improvement in accuracy is also reflected in the percent of patients in which the prediction is within 0.25 D and 0.50 D of subjective refraction (25.8% to 45.5% and 44.7% to 72.9% for 0.25 D and 0.50 D thresholds, respectively).

The most relevant feature for each of the models was the Zernike coefficient associated to the power vector the model was trying to predict: Z_2^0 for the M , Z_2^2 for J_0 , and Z_2^{-2} for J_{45} , as was expected. The second most important parameter considered by all models was the average pupil size during the measurement. This is not surprising considering that pupil diameter is a significant autorefractor feature used to estimate corrective lenses. The third most influential feature was the age, accounting for $\sim 5\%$ of the weight of the prediction. Age is a crucial parameter in datasets containing young children due to factors such as childhood-hyperopia, which in general is very difficult to diagnose due to the high accommodative capacity of children. Specific high-order Zernike coefficients were not relevant for the models, but Z_2^2 was taken into account by the M and J_{45} models. Gender was not considered a remarkable feature by any of the three models.

Decrease in the mean absolute error of the M , J_0 , and J_{45} predictions (0.27 D, 0.06 D, and 0.05 D) for the ASB

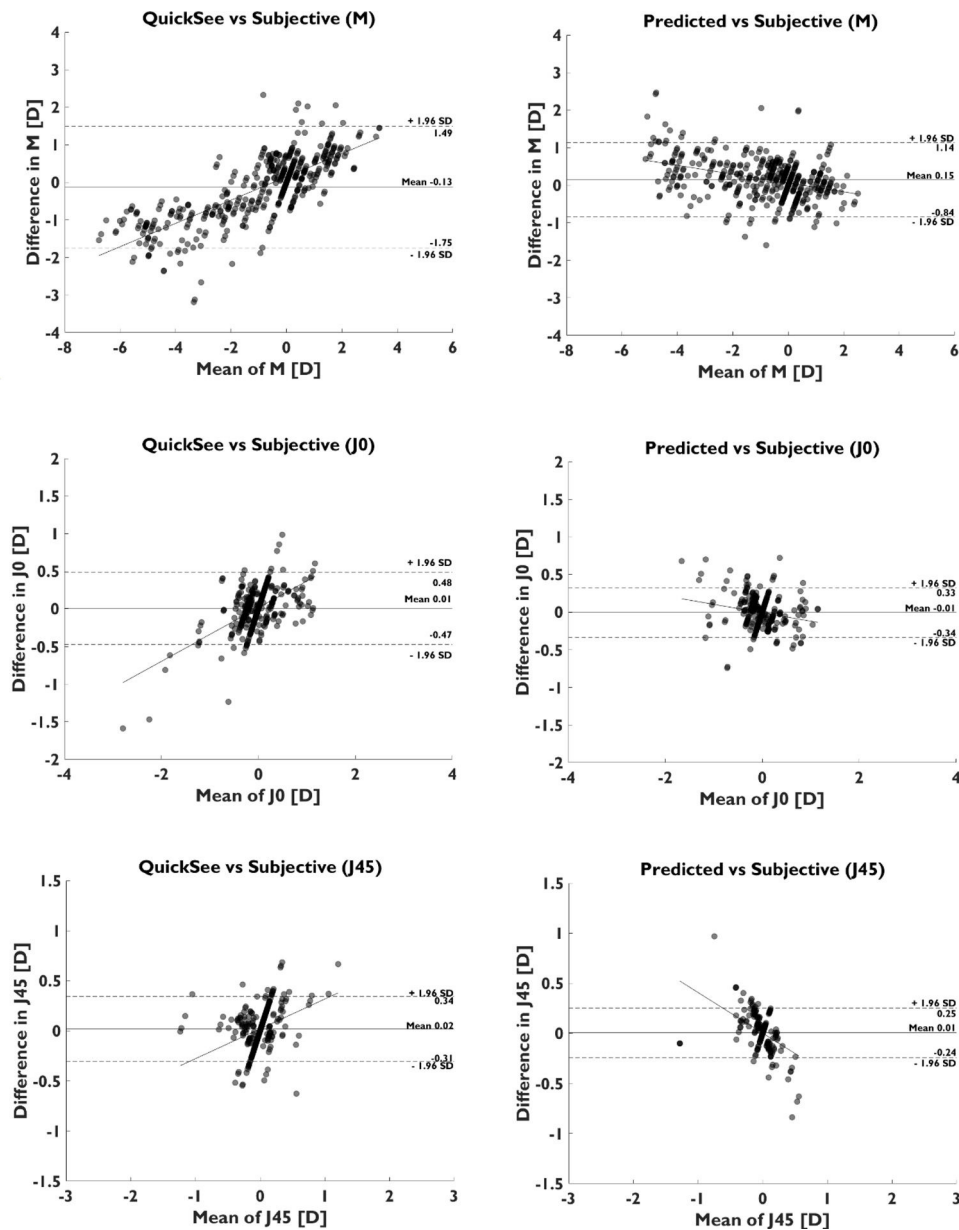


Fig. 3 Bland-Altman plots comparing the agreement between prescriptions provided by the autorefractor (left) and ASB assembly model (right) versus subjective refraction for M , J_0 , and J_{45} .

model was bigger than those values obtained by Rampat et al.²³ using aberrometry data (0.10 D, 0.05 D, and 0.05 D). However, it should be noted that this study was performed under highly controlled conditions using data from a desktop aberrometer, and a new base of polynomials that provide better separation between low- and high-degree wavefront components than standard Zernike polynomials. Apart from these differences, the original error of the baseline model in our study was higher, what could be explained by the heterogeneity in the population characteristics (wider inclusion criteria), and the fact that the instrument used for the study was an early prototype of the current production device operated by a minimally trained technician. Finally, many of the subjects enrolled in this study were emmetropic with 29.56% of the samples within 0.25 D of spherical equivalent. Having a population with a

more heterogeneous refractive error distribution would have been beneficial for the models, but this naturally-occurring distribution has been found to resemble those obtained in other studies.^{43,44}

Results shown in this paper show a considerable improvement in the agreement with SR when compared to the autorefractor predictions obtained by means of the paraxial matching method. An extra validation step would include a comparison of the ASB model against other SR prediction methodologies like image quality metrics^{13,18} or the MTR metric from Jaskulski et al.¹⁹ when executed on the same dataset.

Direct application of these models to patients implanted with multifocal intraocular lenses (IOLs) is not possible due to the limitations of Shack Hartman sensors to separate the overlapping wavefronts

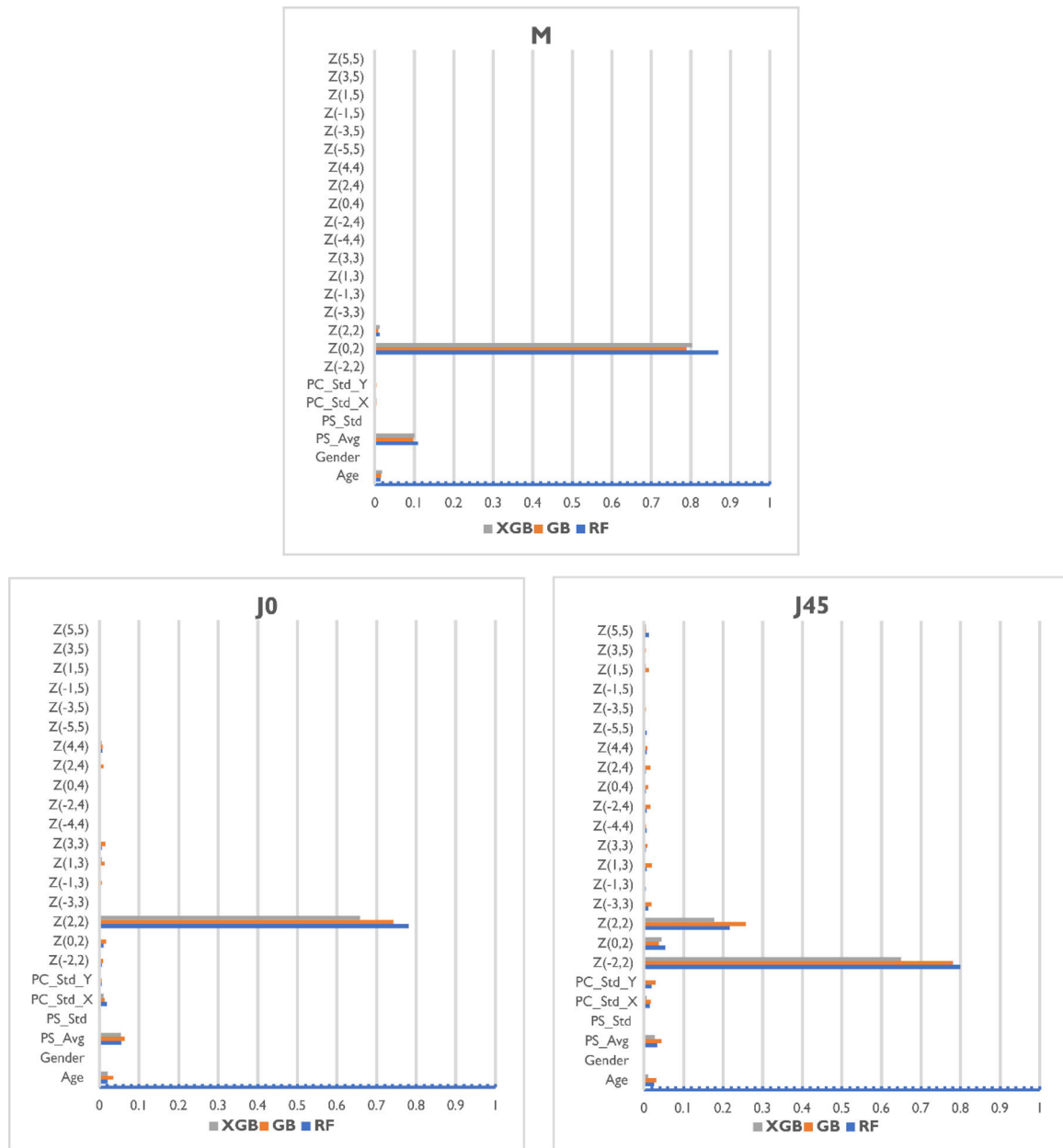


Fig. 4 Permutation-based feature importance of Random Forest (RF), Gradient Boosting (GB), and Extreme Gradient Boosting (XGB) models for predicting the three power vectors M , J_0 , and J_{45} . Permutation values were obtained using a 5-fold crossvalidation on the training set.

generated by the diffractive lenses. A different representation other than the Zernikes would be required, and the models would need extra training and tuning for each specific multifocal IOL.

The results obtained in this work suggest that a ML approach, implementable via software, may potentially improve upon the accuracy of the handheld autorefractor used in the study in a cost-effective manner. An important point to note is that since the most influential variables for the models were the Zernike coefficients, pupil size and age (standard variables in aberrometry), this approach could potentially be extended to other autorefractors, supporting the use of

the proposed methodology to improve access to vision correction by non-technical ECPs in health disparity populations.

Declaration of Competing Interest

E. Lage, S.R. Dave and D. Lim are inventors in patents related to the device presented in this work and have ownership in PlenOptika Inc. A. Gil, C.S. Hernandez, I. Casares and J. Poderoso work or have worked in research and development projects funded by PlenOptika Inc or are employees of this company.

Acknowledgments

Eduardo Lage is funded by the Ramon y Cajal program from the Spanish Ministry of Economy, Industry and Competitiveness (RYC-2016-21125). Jesus Poderoso is funded by the Madrid Regional Government through PEJD-2019-PRE/IND-15478. Carlos S. Hernandez, I. Casares and Andrea Gil are funded by the Madrid Regional Government through IND2019/TIC-17116 and IND2020/TIC-17340 grants. Manuel Sánchez-Montañés is funded by Agencia Estatal de Investigación AEI/FEDER Spain, Project PGC2018- 095895-B-I00, and Comunidad Autónoma de Madrid, Spain, Project S2017/BMD-3688. Research relating to the autorefractor reported in this publication was partially supported by the National Institute of Biomedical Imaging & Bioengineering and National Eye Institute of the National Institutes of Health under Award Numbers R43EB024299 and R44EY025452, respectively. The content is solely the responsibility of the authors and does not necessarily represent the official views of the National Institutes of Health.

References

1. GBD 2019 Blindness and Vision Impairment Collaborators, Vision Loss Expert Group of the Global Burden of Disease Study. Trends in prevalence of blindness and distance and near vision impairment over 30 years: an analysis for the global burden of disease study. *Lancet Glob Health*. 2021;9(2):e130–e143.
2. Steinmetz JD, et al. Causes of blindness and vision impairment in 2020 and trends over 30 years, and prevalence of avoidable blindness in relation to vision 2020: the right to sight: an analysis for the global burden of disease study. *Lancet Glob Health*. 2021;9:e144–e160.
3. Reddy PA, et al. Effect of providing near glasses on productivity among rural Indian tea workers with presbyopia (PROSPER): a randomised trial. *Lancet Glob Health*. 2018;6:e1019–e1027.
4. Smith E, et al. Eyeglasses for global development: Bridging the visual divide. in *World. Economic Forum*. 2016.
5. Burton MJ, et al. The lancet global health commission on global eye health: vision beyond 2020. *Lancet Glob*. 2021. [https://doi.org/10.1016/S2214-109X\(20\)30488-5](https://doi.org/10.1016/S2214-109X(20)30488-5). Health S2214109X20304885.
6. MacKenzie GE. Reproducibility of spherocylindrical prescriptions. *Ophthalmic Physiol Opt*. 2008;28:143–150.
7. Taneri S, Arba-Mosquera S, Rost A, Kießler S, Dick HB. Repeatability and reproducibility of manifest refraction. *J Cataract Refract Surg*. 2020;46.
8. Thibos LN, Applegate RA, Schwiegerling JT, Webb R, & VSIA Standards Taskforce Members. *J. Refract. Surg. Thorofare NJ* 1995 18, S652–660 (2002). <https://doi.org/10.3928/1081-597X-20020901-30>.
9. Huelle JO, et al. Accuracy of wavefront aberrometer refraction vs manifest refraction in cataract patients: impact of age, ametropia and visual function. *Graefes Arch Clin Exp Ophthalmol*. 2013;251:1163–1173.
10. Pesudovs K, Parker KE, Cheng H, Applegate RA. The precision of wavefront refraction compared to subjective refraction and autorefraction. *Optom Vis Sci*. 2007;84:387–392.
11. Visser N, et al. Evaluation of the comparability and repeatability of four wavefront aberrometers. *Investig Ophthalmology Vis Sci*. 2011;52:1302.
12. Guirao A, Porter J, Williams DR, Cox IG. Calculated impact of higher-order monochromatic aberrations on retinal image quality in a population of human eyes: erratum. *J Opt Soc Am A*. 2002;19:620.
13. Chen L, Singer B, Guirao A, Porter J, Williams DR. Image metrics for predicting subjective image quality. *Optom Vis Sci*. 2005;82:358–369.
14. Teel DFW, Jacobs RJ, Copland J, Neal DR, Thibos LN. Differences between wavefront and subjective refraction for infrared light. *Optom Vis Sci*. 2014;91:1158–1166.
15. Li YJ, Choi JA, Kim H, Yu SY, Joo CK. Changes in ocular wavefront aberrations and retinal image quality with objective accommodation. *J Cataract Refract Surg*. 2011;37:835–841.
16. Mon-Williams M, Tresilian JR, Strang NC, Kochhar P, Wann JP. Improving vision: neural compensation for optical defocus. *Proc R Soc Lond B Biol Sci*. 1998;265:71–77.
17. Artal P, et al. Neural compensation for the eye's optical aberrations. *J Vis*. 2004;4:4.
18. Cheng X. Predicting subjective judgment of best focus with objective image quality metrics. *J Vis*. 2004;12.
19. Jaskulski M, Martínez-Finkelstein A, López-Gil N. New objective refraction metric based on sphere fitting to the wavefront. *J Ophthalmol*. 2017;1–9. 2017.
20. Hastings GD, Marsack JD, Nguyen LC, Cheng H, Applegate RA. Is an objective refraction optimised using the visual strehl ratio better than a subjective refraction? *Ophthalmic Physiol Opt*. 2017;37:317–325.
21. Guo Y, Hao Z, Zhao S, Gong J, Yang F. Artificial intelligence in health care: bibliometric analysis. *J Med Internet Res*. 2020;22:e18228.
22. Leube A, Leibig C, Ohlendorf A, Wahl S. Machine learning based predictions of subjective refractive errors of the human eye. In: *Proceedings of the 12th International Joint Conference on Biomedical Engineering Systems and Technologies*. 199–205, SCITEPRESS - Science and Technology Publications; 2019. <https://doi.org/10.5220/0007254401990205>.
23. Rampat R, Debellemanière G, Malet J, Gatinel D. Using artificial intelligence and novel polynomials to predict subjective refraction. *Sci Rep*. 2020;10:8565.
24. Gatinel D, Malet J, Dumas L. Polynomial decomposition method for ocular wavefront analysis. *J Opt Soc Am A*. 2018;35:2035–2045.
25. Ostadimoghaddam H, et al. Prevalence of the refractive errors by age and gender: the Mashhad eye study of Iran: refractive errors in Mashhad, Iran. *Clin Exp Ophthalmol*. 2011;39:743–751.
26. Durr NJ, et al. Quality of eyeglass prescriptions from a low-cost wavefront autorefractor evaluated in rural India: results of a 708-participant field study. *BMJ Open Ophthalmol*. 2019;4.
27. Durr NJ, et al. Design and clinical evaluation of a handheld wavefront autorefractor. *Optom Vis Sci*. 2015;92:1140–1147. *Off Publ Am Acad Optom*.
28. Durr, N. J. et al. Apparatus and Method of Determining an Eye Prescription. US20160128562A1, May 12, (2016).
29. Zheng A, Casari A. Feature engineering for machine learning: principles and techniques for data scientists. O'Reilly Media, Inc; 2018.
30. Hastie T, et al. The elements of statistical learning: data mining, inference, and prediction. *The Elements of Statistical Learning*. New York: springer; 2009.
31. *Ensemble Machine Learning*. Springer US; 2012. <https://doi.org/10.1007/978-1-4419-9326-7>.
32. Natekin A, Knoll A. Gradient boosting machines, a tutorial. *Front Neuroinformatics*. 2013;7.
33. Chen T, Guestrin C. XGBoost: a scalable tree boosting system. In: *Proceedings of the 22nd ACM SIGKDD International Conference on Knowledge Discovery and Data Mining*. 2016:785–794. <https://doi.org/10.1145/2939672.2939785>.

34. Thibos L, Wheeler W, Horner D. Power vectors: an application of Fourier analysis to the description and statistical analysis of refractive error. *Optom Vis Sci.* 1997;74:367–375.
35. McAlinden C, Khadka J, Pesudovs K. Statistical methods for conducting agreement (comparison of clinical tests) and precision (repeatability or reproducibility) studies in optometry and ophthalmology. *Ophthalmic Physiol Opt.* 2011;31:330–338.
36. Fernández de Castro LE, Sandoval HP, Bartholomew LR, Vroman DT, Solomon KD. High-order aberrations and preoperative associated factors. *Acta Ophthalmol Scand.* 2006;85:106–110.
37. Mathur A, Gehrman J, Atchison DA. Influences of luminance and accommodation stimuli on pupil size and pupil center location. *Investig Ophthalmology Vis Sci.* 2014;55:2166.
38. Kang P, Swarbrick H. Peripheral refraction in myopic children wearing orthokeratology and gas-permeable lenses. *Optom Vis Sci.* 2011;88:476–482.
39. Sankaridurg P, et al. Myopia control with novel central and peripheral plus contact lenses and extended depth of focus contact lenses: 2 year results from a randomised clinical trial. *Ophthalmic Physiol Opt.* 2019;39:294–307.
40. Lockhart TE, Shi W. Effects of age on dynamic accommodation. *Ergonomics.* 2010;53:892–903.
41. Shufelt C, Fraser-Bell S, Ying-Lai M, Torres M, Varma R. Refractive error, ocular biometry, and lens opalescence in an adult population: the Los Angeles latino eye study. *Investig Ophthalmology Vis Sci.* 2005;46:4450.
42. Orucoglu F, Akman M, Onal S. Analysis of age, refractive error and gender related changes of the cornea and the anterior segment of the eye with scheimpflug imaging. *Contact Lens Anterior Eye.* 2015;38:345–350.
43. Raju P, et al. Prevalence of refractive errors in a rural South Indian population. *Invest Ophthalmol Vis Sci.* 2004;45:4268–4272.
44. Natung T, Taye T, Lyngdoh LA, Dkhar B, Hajong R. Refractive errors among patients attending the ophthalmology department of a medical college in North-East India. *J Fam Med Prim Care.* 2017;6:543.